Journal of Applied Polymer Science

Numerical Simulation Study of the T-Peel Behavior of Coated Fabric Films Used in Inflatable Structures

Yabin Yang, Pan Zeng, Liping Lei
Department of Mechanical Engineering, Tsinghua University, 307B Hanjieguan Building, Qinghua Yuan, Haidian District, Beijing 100084, People's Republic of China
Correspondence to: P. Zeng (E-mail: zengp@mail.tsinghua.edu.cn)

ABSTRACT: A simple and reliable finite element method was developed to analyze the T-peel behavior of fabric coated with thin films. The material model was constructed simply by a tensile test of the coating and the coated fabric. In addition, the influence of the welding parameters on the mechanical properties of the welded zone was considered. Although some material characters were neglected, the material model was found to be convenient for engineering applications. The reliability was examined by a comparison of the numerical results with the experiments. A T-peel test was conducted, and a camera configured with an optical microscope lens was used to observe the material flow from the thickness view. The load–displacement curve predicted by the simulation agreed well with the experimental results. Small voids were detected when the sample was near fracture. These places were consistent with the simulation results and showed where the maximum stress–strain was located. © 2014 Wiley Periodicals, Inc. J. Appl. Polym. Sci. **2015**, *132*, 41299.

KEYWORDS: adhesives; applications; fibers; films; theory and modeling

Received 5 May 2014; accepted 15 July 2014
DOI: 10.1002/app.41299

INTRODUCTION

Inflatable structures have received considerable attention in recent decades for the advantages of its light weight, lower cost, convenience to transport, easier deployment, and so on.[1] Mostly, inflatable structures are thin-film structures constructed with simple lap seams, and these seams are the lowest strength components in the whole structure. For the lap seams, the shear-mode loading has much more strength than the peel-mode loading, as shown in Figure 1. Unfortunately, peel-mode loading must exist for machine-manufactured airtight airbags (except the seamless ones), so the T-peel test is a commonly used method for testing the seam strength,[2] as shown in Figure 2(a). When the lap seams are peeled as the structure is inflated, the deformation surrounding the seam area is inhomogeneous; this is the main reason for wrinkling there. Hence, the investigation of the deformation surrounding the seam area is very important for the shape control of the inflatable structure. Nase et al.[3] investigated the peel process with environmental scanning electron microscopy. Although the deformation process can be understood comprehensively, the stress–strain condition cannot be obtained directly. Yang et al.[4] observed the T-peel behavior by a noncontact measurement, digital image correlation (DIC), to obtain the strain field. As shown in Figure 2(b), the outermost layer of the T-peel sample was sprayed with randomly distributed black and white speckles. Different areas of the outermost layer were identified by different grayscale values, and thus, the deformation of the outermost layer could be recognized and traced by the two cameras. After some data processing, the fulfilled strain of the outmost layer could be obtained. However, only the outermost layer stain could be measured, and there were no strain data along the thickness direction. The thickness of the sample was very thin; hence, it was very difficult to spray appropriate speckles and record the deformation with normal cameras. Furthermore, the seam was very narrow, so the cameras may not have been useful to obtain the deformation details within the seam. Moreover, there were negative strains observed in the experiment, and it was insufficiently explained.

Therefore, finite element (FE) analysis is another common method of studying the complex stress–strain distribution of the T-peel system. It is of interest to many researchers to investigate the steady-state peeling process after fracture initiation with the FE method.[5–7] However, in this study, we focused on the transient peeling process before fracture initiation because the entire inflatable structure would fail because of the gas leakage if fracture had occurred, so the investigation of the transient peeling process was more meaningful.

One problem for the FE analysis is how to construct the appropriate material model. Inflatable structures are usually produced from a flexible composite material consisting of a fabric

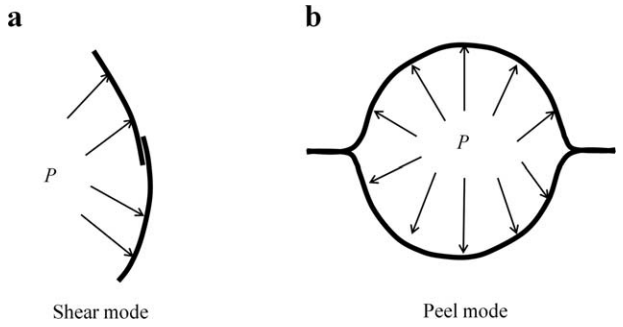

Figure 1. Two loading modes for the lap seams as the structure was inflated: (a) shear mode and (b) peel mode.

reinforcement material coated with an airtight sealant on one or both sides. The fabric increases the load-bearing ability, and the coating prevents gas leakage. Many researchers have worked to develop a refined model of this composite[8–10] and have tried to take into account as many as possible of the material physical properties into their models, such as the number of the warp and weft yarns, the distance and friction between them, and the friction between the fabric and the coating. Pargana et al.[11] gave a review of the existing models of fabric and proposed a novel fabric model, in which they gave full consideration to the true behavior of the fabrics. There were 15 model parameters that needed to be determined. Despite their model being accurate and reliable, the large number of parameters makes it inconvenient for engineering applications. Hence, a simple and feasible FE material model without a loss in accuracy needs to be developed for engineering use.

Another problem is how to take into account the influence of processing parameters on the mechanical properties of the seam. High-frequency (HF) welding or HF dielectric heating is a widely used method for joining these flexible films together.[12] The coatings are melted under the HF electromagnetic field and then fused together.[13] As some coatings are squeezed out at the end the welded zone because of the applied welding pressure, the welded zone shows a concave appearance. This phenomenon leads to the peeling angles of the upper and lower peeling arm (ϕ_u and ϕ_l, respectively) not being 90°, as shown in Figure 2, but they vary with the welding parameters. Thus, the initial geometric model of the T-peel sample was somewhat difficult to determine. In addition, it was also necessary to investigate whether the constitutive law of the melted and remixed coatings was changed because of welding.

Therefore, in this study, we were motivated to resolve the previous two problems. A T-peel test was first undertaken to assess the influence of the welding parameters on the mechanical response of the welded samples, and a camera with an optical microscope lens was used to observe the material flow from the thickness cross-sectional view. We found that the welding process caused little change to the constitutive law of the welded region. Then, a convenient and reliable FE method was proposed to simulate the T-peel test. The simulation results and the experimental observations had perfect agreement. The simulation results were also compared with the work of Yang et al.,[4] who used the DIC technique to obtain the T-peel strain field.

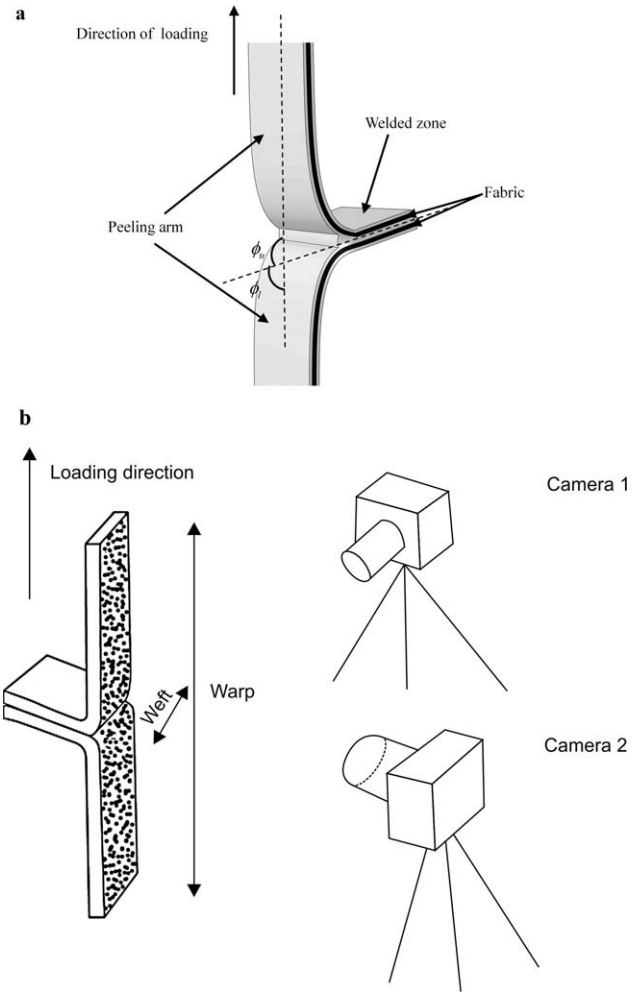

Figure 2. (a) T-peel test. (b) The deformation of the sample was recorded by two cameras, and then, the images were used to obtain the fulfilled strain with DIC.[4]

The remainder of this article is organized as follows. The Experimental section details the material, HF welding process, and the T-peel test. The Results and Discussion section discusses how the welding parameters influenced the fracture mode and T-peel load–displacement curve. The Numerical Simulation section introduces the FE method and gives an analysis the numerical results in detail. The article concludes with a reiteration of the most salient points of this study in the Conclusions section.

EXPERIMENTAL

Materials

The material used in this study was plain-weave nylon fabric coated on both sides with white thermoplastic polyurethane (TPU) elastomers because this material is widely used to fabricate inflatable structures,[12] such as the inflatable architectures, airships, and other aerospace applications. The total thickness of the TPU-coated fabric was 0.6 mm, and its cross section is shown in Figure 3(a). The tensile stress–strain relationship of the nylon fabric was orthotropic because it was woven with orthogonally oriented intertwined yarns, as shown in Figure 3(b). The axially oriented yarns were referred to as warp yarns,

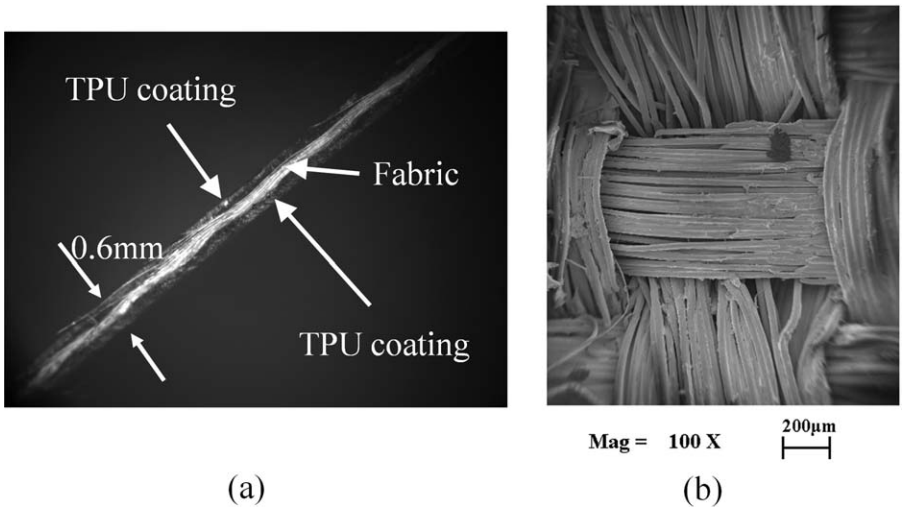

Figure 3. (a) TPU-coated fabric and (b) nylon fabric.

and the hoop-oriented ones were known as weft yarns.[1] The TPU coating was isotropic, and its stress–strain behavior was similar to that of the rubber, which is often modeled as hyperelastic. The coated fabric was stored in rolls at ambient temperature, and the welding samples were directly cut from the rolls.

HF Dielectric Heating and T-Peel Test

An HF dielectric heating apparatus was used to weld the samples together with various settings of the welding parameters, and then, the welded sample was subjected to the T-peel test. The welding process is shown schematically in Figure 4(a). The

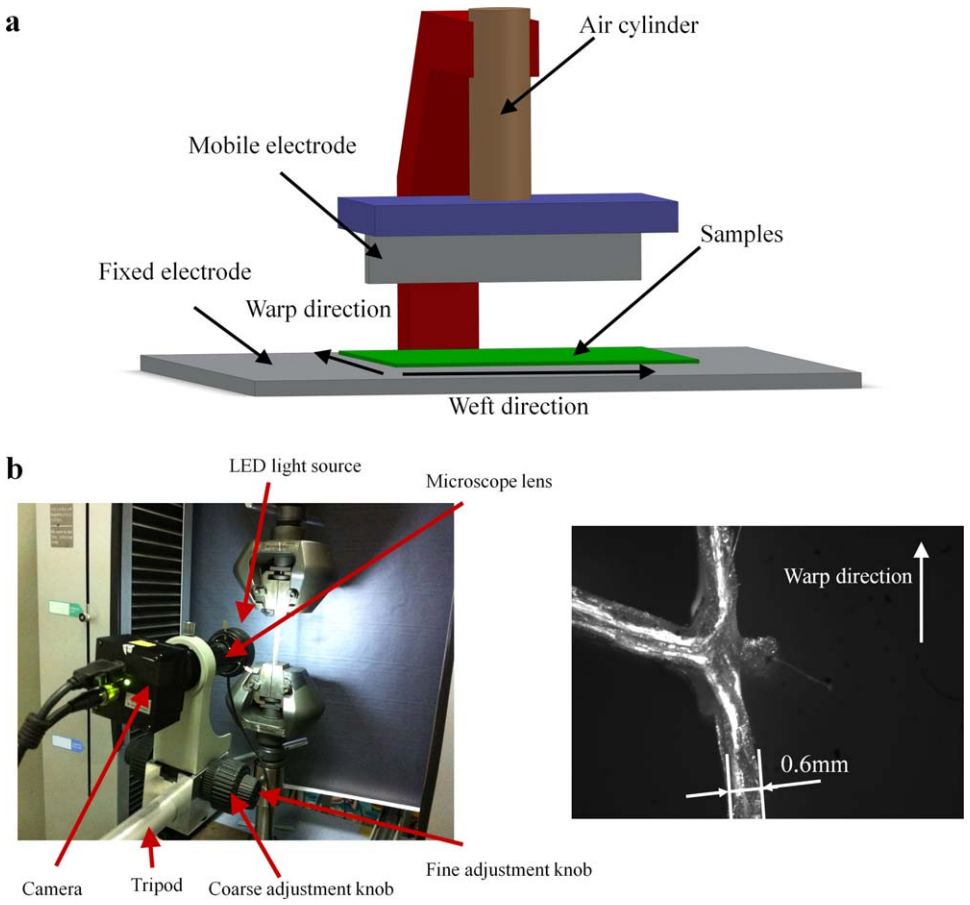

Figure 4. (a) Schematic of the HF dielectric heating apparatus. (b) A camera configured with an optical microscope lens was used to observe the T-peel test from the thickness view. [Color figure can be viewed in the online issue, which is available at wileyonlinelibrary.com.]

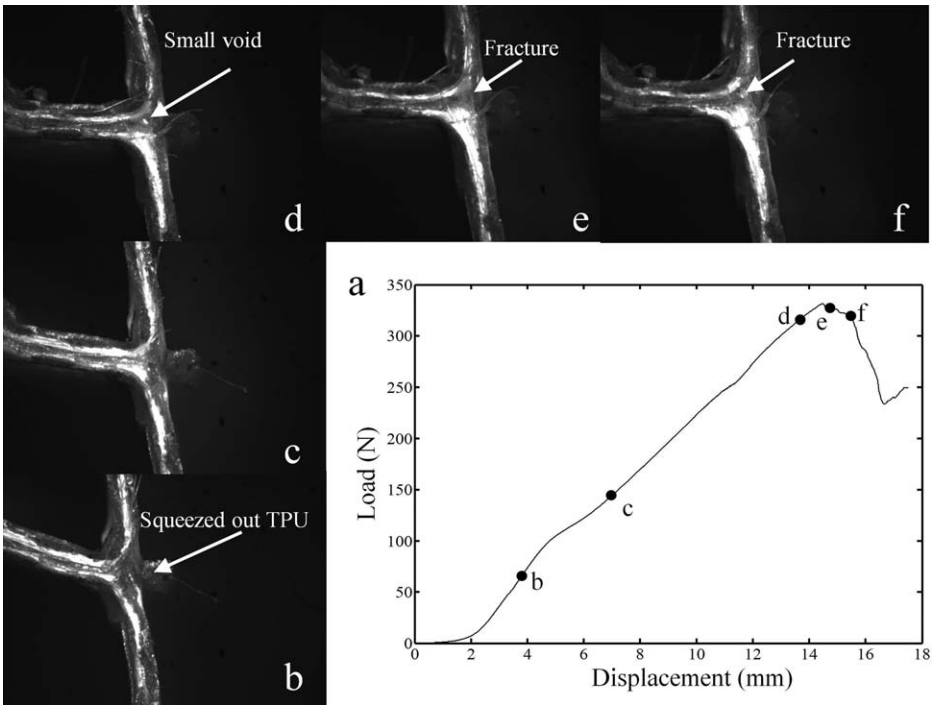

Figure 5. (a) Typical peel load–displacement curve and (b–f) the corresponding images at different positions of the peel process.

electrodes were used to supply HF energy in the form of 27.12 MHz. The sample warp yarns were oriented along the thickness direction of the mobile electrode. The T-peel test was performed on a Shimadzu universal tester. The gauge length was 600 mm, and the peel rate was 3 mm/min. The loading direction was parallel to the warp yarns. A camera (Daheng Image, China) configured with an optical microscope lens, as shown in Figure 4(b), was used to observe the entire peeling process from the thickness view.

RESULTS AND DISCUSSION

A typical load–displacement relationship of the welded sample and the corresponding peeling process captured by the microscope camera are shown in Figure 5. Because the reflective rate of the fabric and TPU were different, they can be clearly distinguished from the images; the whiter part was the fabric. In Figure 5(b), it can be seen that ϕ_u and ϕ_l were not 90° at the beginning of the T-peel test. This was caused by the different thicknesses of the peeling arm and the welded zone.[4] As the load increased, the peeling angles gradually grew to 90°, and the deformation at the end of the welded zone (or at the root of the peeling arm) became larger. The squeezed-out part of the TPU barely deformed. When the sample was near to fracture, there was a small void observed, as shown in Figure 5(d). As shown in Figure 5(e,f), the small void grew larger and fractured; the TPU coatings were torn away from the fabric.

Actually, there were three different failure modes with the change of the welding parameters, as shown in Figure 6. In the first mode, the joined TPU coatings were torn away, and this was called intralaminar fracture, as shown in Figure 6(a). For this mode, it was usual that the heat produced at the welding interface was not sufficient to make the TPU coatings mix adequately, and the fracture force was very low. The second mode was when the melt point was achieved, and the melted TPU coatings were mixed with each other more adequately under the pressure. Fracture occurred at the interface of the coating and the fabric, which was called interlaminar fracture, as shown in Figure 6(b). The third mode was when the heat and welding pressure grew further, and the strength of the welded zone exceeded that of the parent material, with a failure mode in which the parent material (including the fabric and the coatings) surrounding the welded zone was torn away, as shown in Figure 6(c). This mode had the highest fracture force and was called fiber fracture. If we continued to increase the heat,

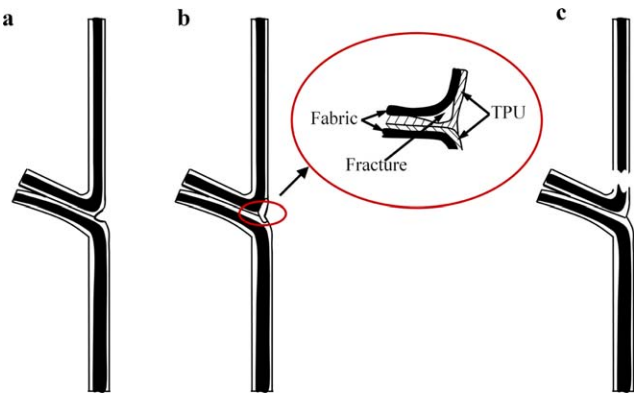

Figure 6. (a) Intralaminar fracture, (b) interlaminar fracture, and (c) fiber fracture. [Color figure can be viewed in the online issue, which is available at wileyonlinelibrary.com.]

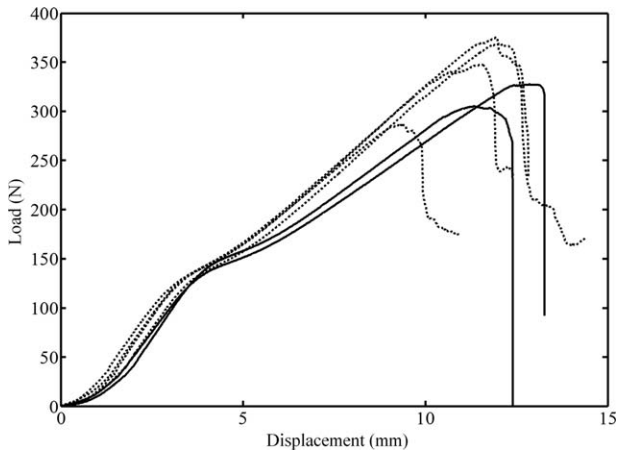

Figure 7. Peel load–displacement curves with various welding parameters.

although the failure mode was still fiber fracture, the fracture force decreased rapidly. This was because too much heat would induce a significant heat-affected zone and seriously deteriorate the parent material surrounding the welded zone.

The peel load–displacement curves with different welding parameters are shown in Figure 7. The solid lines represent the samples welded with too much heat, and the parent material was seriously deteriorated. This condition is generally not acceptable in welding practice; thereby, it was not considered in this study.

The dashed lines in Figure 7 indicated that the HF welding process had little influence on the constitutive law of the welded material when the welding parameters were appropriate. Despite the failure modes and corresponding failure forces being different with various welding parameters, the load–displacement curves before fracture were similar. Thus, in the numerical simulation study, the stress–strain relationship of the welded zone could be assumed to be the same as that of the parent material.

NUMERICAL SIMULATION

FE Modeling

In the experiments conducted by the Yang et al.[4] and Nase et al.,[3] the melted TPU coatings moved toward the border of the welded zone during welding, and thus, the cross section of the seal area gained a concave appearance after welding, as shown in Figure 8(a). This caused an angle between the two peeling arms (α), and hence, the peel angles were not 90° at the beginning of the T-peel test but varied with the change in the welding parameters. In addition, for the flexible polymers, there was some initial stress at the beginning of the T-peel test. To construct the initial state of the T-peel test precisely, the geometric model of the welded sample was constructed first, and a certain α was given. The squeezed-out part of the TPU coatings at the end of the welded zone was also constructed in the model, as shown in Figure 8(b). Because the experimental results showed that the welded samples with a different α exhibited similar load–displacement relationships, α was not a sensitive parameter to the numerical results. Thus, in this study, α was set to be 30°. The simulation study was performed on ABAQUS, and the simulation process was divided into two steps: In the first step, the end of the lower peeling arm was fixed, and a small force of about 5 N was applied at the end of the upper peeling arm, as shown in Figure 9(a). By a steady-state analysis, the initial geometric model of the T-peel test was obtained, as shown in Figure 9(b). In the second step, the force boundary condition at the end of the upper peeling arm was deactivated, and instead, a velocity boundary condition was applied. The velocity in the y direction was set to be 3 mm/min, and the velocities in the x direction and z direction were set to be 0.

The nominal stress–strain relationship of the TPU coating and the load–displacement curve of the 20 × 0.6 mm^2 TPU-coated fabric with a 40 mm long gauge are shown in Figure 10(a,b), respectively. The data was obtained by uniaxial tension tests. The constitutive law of the TPU coating was modeled as hyperelastic. With the ABAQUS software, the material model was evaluated with the stress–strain data, as shown in Figure 10(a). The major finding was the second order of the Ogden material model could best describe the TPU coating constitutive law.

The fabric stress–strain relationship was dependent on many factors, such as the weaving method, the number of warp and weft yarns, and the friction between them. Thus, it is usually difficult to describe the constitutive law of the weave fabric. Here, a simplified method was used to obtain the fabric stress–strain relationship. The essential points are presented here.

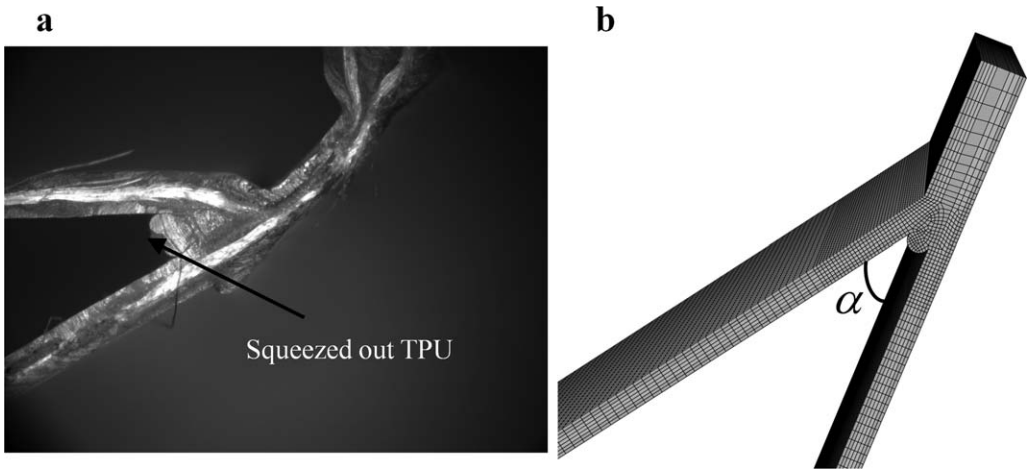

Figure 8. (a) Sample after welding and (b) FE geometric model of the welded sample.

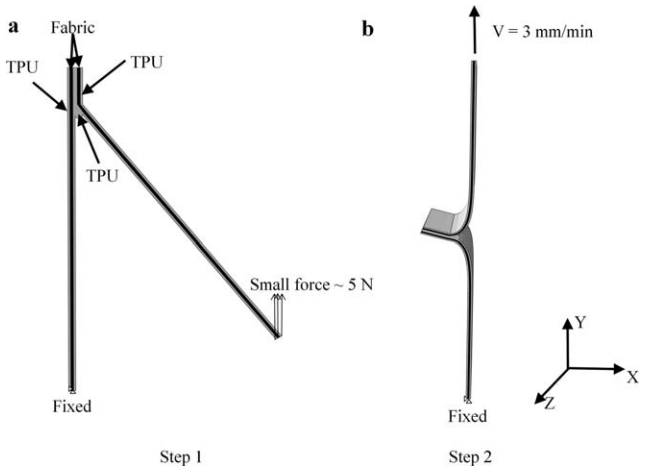

Figure 9. The simulation process was divided into two steps: (a) the first step was used to obtain the initial state of the T-peel test, and (b) the second step was used to simulate the T-peel process. V represented the peel rate.

For the uniaxial tension test of the TPU-coated fabric, the strains of the TPU coating and the fabric were assumed to be identical because no obvious relative sliding between them was observed. This assumption agreed well with the experimentally obtained data in ref. 4. The nominal stress value of the TPU coatings ($\sigma_{n,T}$) and the nominal stress value of the fabric ($\sigma_{n,F}$) satisfied the following equation:

$$F=\sigma_{n,T}bh_T+\sigma_{n,F}bh_F \tag{1}$$

where F is the tensile load, b is the width, and h_T and h_F are the thicknesses of the TPU coatings and fabric, respectively. As shown in Figure 10(a), the load-bearing ability of TPU was weak compared with that of the fabric. The load that the TPU bore was no more than 10 MPa when the strain was less than 1. This area was defined as the low-load-bearing zone. The load increase rate grew rapidly with the increasing strain, and this area was defined as the high-load-bearing zone. The exact breakpoint of the low-load-bearing zone and the high-load-bearing zone was difficult to define, and the point when the strain was equal to 1 was just a general segment for the load–displacement curve. For the uniaxial tension test of the TPU-coated fabric, the nominal strain was no more than 1, and thus, the TPU coating was in the low-load-bearing zone. Therefore, the fabric bore most of the load, and the contribution of the TPU coating to the load could be neglected. According to eq. (1), the true stress of the fabric ($\sigma_{t,F}$) can be given by

$$\sigma_{t,F}=\frac{F}{bh_F}(1+\varepsilon_n) \tag{2}$$

where ε_n is the nominal strain. With the load–displacement of the TPU-coated fabric and eq. (2), the fabric stress–strain relationship could be obtained; the true stress–strain curves are shown in Figure 10(c), and they can be described as follows:

$$\sigma_{t,F}=\begin{cases} E\varepsilon_t \text{ if} \sigma_{t,F}\le\sigma_0 \\ \dfrac{\sigma_0}{\varepsilon_0}\varepsilon_t^n \text{ if} \sigma_{t,F}\ge\sigma_0 \end{cases} \tag{3}$$

where n is a material parameter. ε_t is the true strain, σ_0 is the yield stress, ε_0 is the yield strain, and E is the Young's modulus.

The plain-weave nylon fabric was modeled as orthotropic. The shear modulus was estimated with the following equation, which was recommended by the International Association for Shell and Spatial Structures (IASSS):[14]

$$\frac{1}{G_{ij}}=\frac{4}{E_{ij,45^\circ}}-\frac{1}{E_i}-\frac{1}{E_j}+\frac{2v_{ij}}{E_i},\ i,j=\ 1,2,3 \tag{4}$$

where i or $j=1$, 2, 3 represent the warp direction, the weft direction, and the direction perpendicular to the warp and weft yarns, respectively. G_{ij} means the shear modulus. $E_{ij,45^\circ}$ means the modulus along the direction, which was 45° to the i and j direction. E_1, E_2, and $E_{12,45^\circ}$ were obtained by the uniaxial tension test. E_3 and $E_{i3,45^\circ}$ were likely to be very small for the

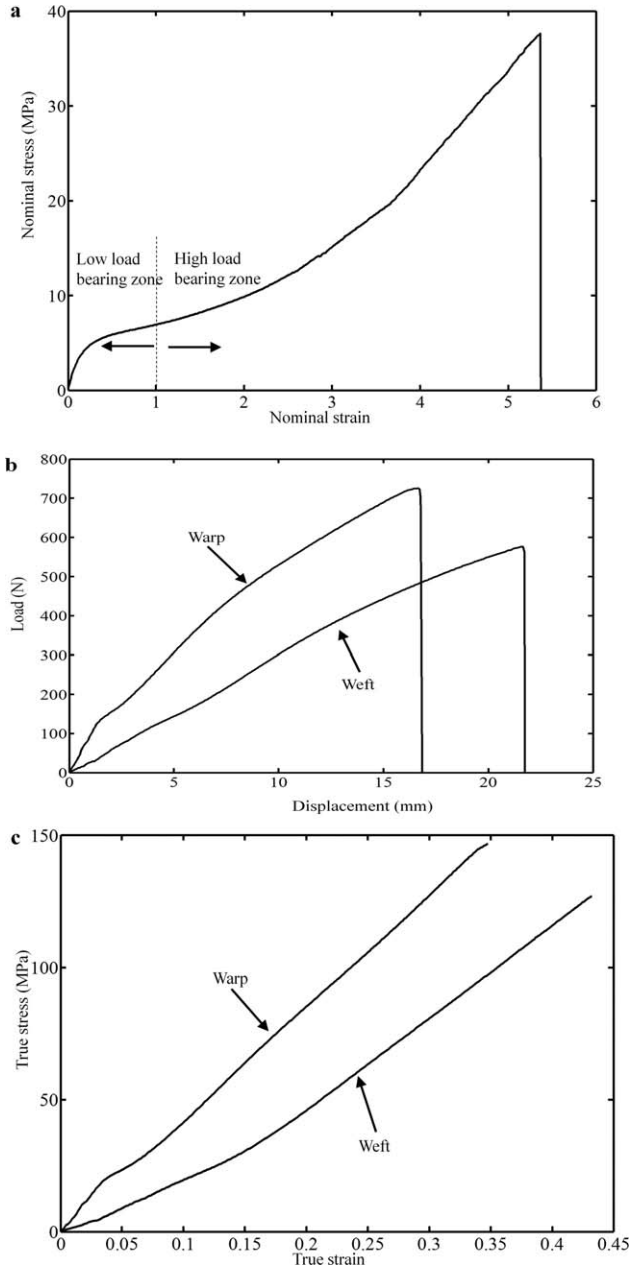

Figure 10. (a) Nominal stress–strain relationship of the TPU coating. (b) Load–displacement relationship of the TPU-coated fabric. (c) True stress–strain relationship of the fabric.

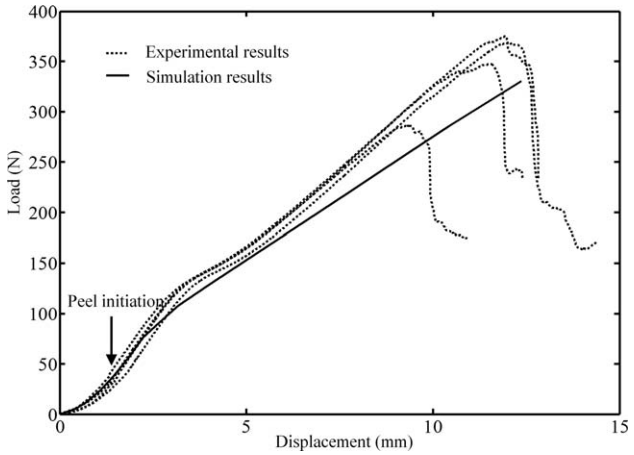

Figure 11. Simulation load–displacement curve compared with the experimental results.

flexible film and were assumed to be one-third of E_1. v_{ij} was set to be 0.5 on the basis of an assumption of volume invariance. The values of E_3 and $E_{i3,45^\circ}$ were based on trial and error. We found that the simulation results were not sensitive to E_3, $E_{i3,45^\circ}$, and v_{ij}. The modulus along the warp and weft directions (E_1 and E_2) were the main parameters influencing the results.

The reason that TPU exhibits hyperelasticity is that it is composed of hard and soft segments.[12,15] At room temperature, the soft segments, which are above their glass-transition temperature, impart the material its rubberlike behavior. The hard segments are below their glass-transition temperature and are thought to govern the hysteresis, permanent deformation, high modulus, and tensile strength.[15] Thus, TPU was described as "bridging the gap between rubber and plastics" by the Alliance for the Polyurethane Industry because it offers the mechanical performance characteristics of rubber but can be processed as a thermoplastic.[15]

Nylon is made of repeating units linked by amide bonds and is frequently referred to as polyamide. At the beginning of the tensile test, the molecular chain of the polyamide was elongated. Then, when it achieved the elastic limit, the molecular structure reoriented; thus, the load increased more slowly with increasing displacement than in the previous stage, as shown in Figure 10(b,c). When the molecular reorientation was finished, the molecular chain was elongated again, and the load increased rapidly. This process made the coated fabric show similar hyperelasticity as the TPU coating.

It should be noted that both the TPU coating and the nylon fabric exhibited plasticity behavior. It was more accurate to describe their stress–strain relationship in terms of elastic and plastic deformation; thus, the constitutive law of the fabric was described with eq. (3). However, the deformation of the TPU was very large at the root of the peeling arm. When the TPU was also modeled with eq. (3), for an implicit computation, the mesh was seriously distorted when the load was greater 200 N, and this caused a nonconvergent problem. Although an explicit computation could solve the problem, it would take much more computation time. When the TPU was modeled as hyperelastic, the nonconvergent problem could be perfectly solved. Furthermore, during the T-peel process, unloading phenomenon only occurred for the bent part at the beginning the test;[4] hence, the plastic deformation was very small and did not cause much calculation error. Therefore, the hyperelastic model was a good simplification for the TPU coating.

Numerical Results and Discussion

As shown in Figure 11, the simulation load–displacement curve of the T-peel test closely mirrored the experimental results. This proved that the numerical method was an effective way to analyze the T-peel test of the flexible composite films. The initial von Mises stress and logarithmic strain state of the T-peel sample are shown in Figure 12. The maximum stresses, measured at about 30 MPa, were at the interface of the fabric and TPU

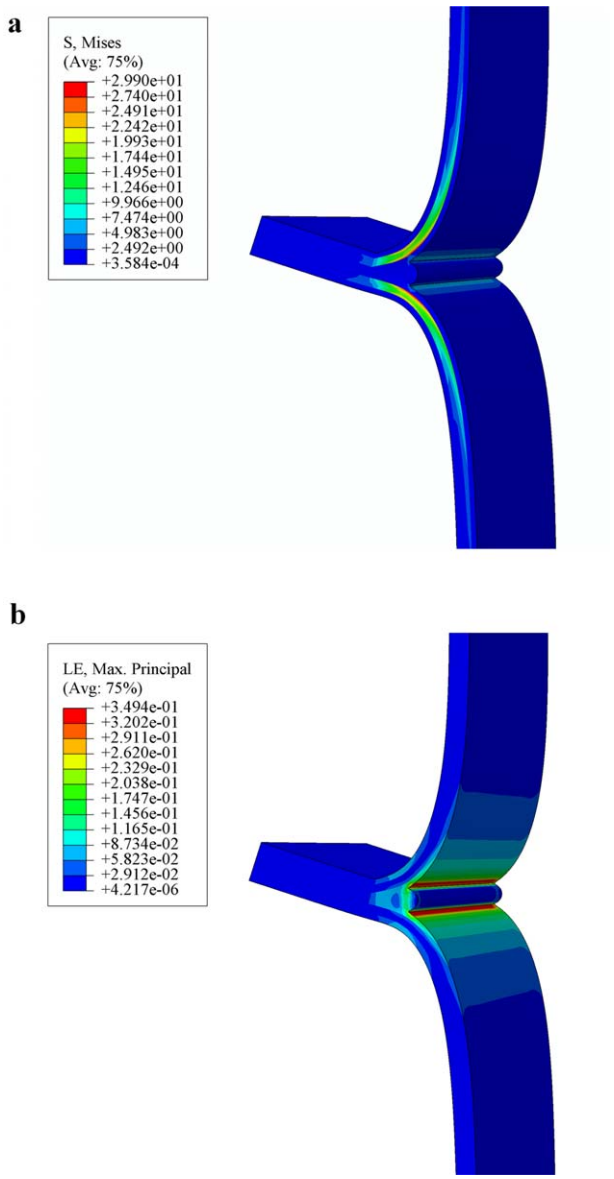

Figure 12. (a) Stress and (b) strains at the beginning of the T-peel test. S means the von Mises stress, LE means the logarithmic strain. [Color figure can be viewed in the online issue, which is available at wileyonlinelibrary.com.]

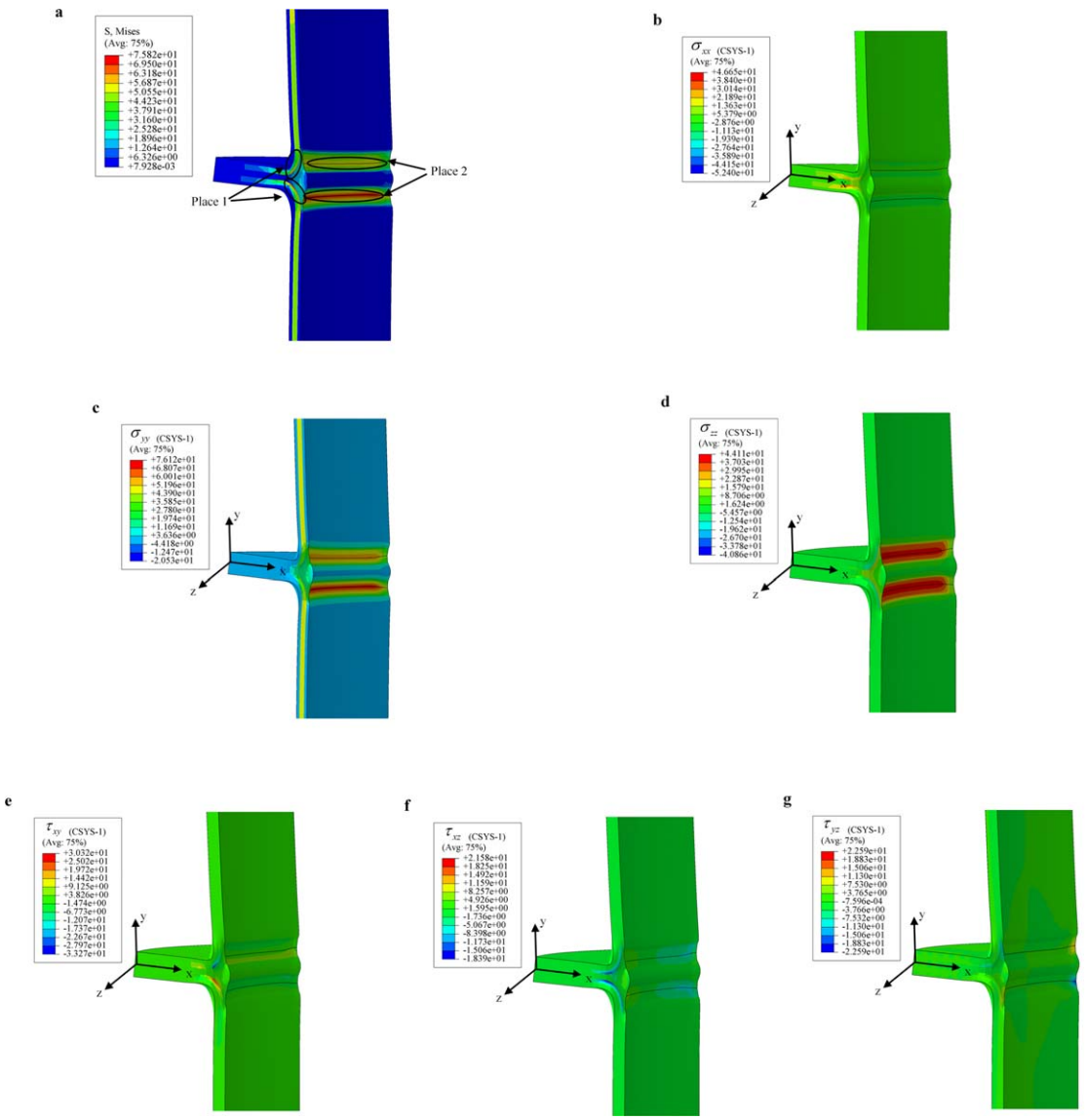

Figure 13. (a) von Mises stress and (b–g) corresponding stress components when the load was about 250 N. τ means the shear stress. CSYS-1 means the rectangular coordinate system shown in the Fig. 13(b) - Fig. 13(g). [Color figure can be viewed in the online issue, which is available at wileyonlinelibrary.com.]

coatings, which was at the root of the peeling arm. The maximum initial strain was about 0.35 and occurred at the joint of the welded zone and the parent material. Figure 13(a) shows the stress condition when the load was about 250 N. Both place 1, where the fabric interfaced with the TPU at the root of the peeling arm, and place 2, where the joint of the welded zone and the parent material were located, had much larger stresses than other places. The TPU coatings at place 2 moved into the high-load-bearing zone and thus could bear large stresses. The TPU coatings in other areas bore little loads. Figure 13(b–g) shows the nephograms of different stress components. The *y*-direction stress dominated in the peeling arm, whereas the *x*-direction stress dominated in the welded zone, where it was near the root of the peeling arm. The joints of the welded zone and the parent material bore much more *z*-direction stress because the materials there shrunk along the *z* direction under the peel load. This shrinking phenomenon was the reason for the wrinkles occurring within the area surrounding the seam of the inflatable structure. The shear stresses concentrated at the interface of the fabric and TPU coatings, which was at the root of the peeling arm. Their values were about one-half to one-quarter of the corresponding normal stress.

The peeling arm could be roughly divided into the bent part and the straight part, as shown in Figure 14. During the peel process, the simulation result shows there was a local unloading phenomenon for the bent part because of the straightening effect. However, there was no unloading phenomenon surrounding the joint of the welded zone and the parent material. The moment when the local unloading occurred was the exact moment of peel initiation, which was defined by Nase[3] and is shown in Figure 11. These results were consistent with the experimental results in ref. 4, in which the strain distribution

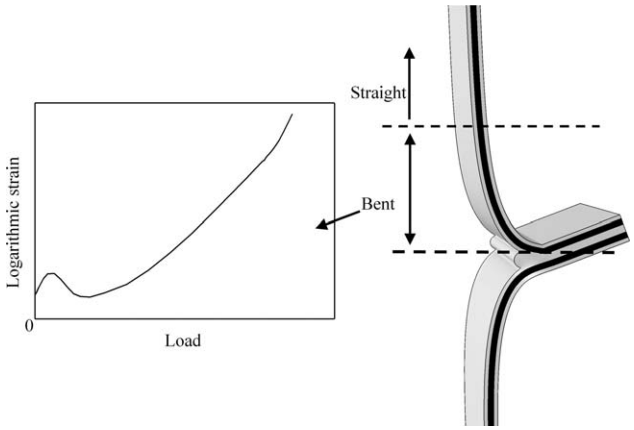

Figure 14. Local unloading phenomenon for the bent part of the peeling arms.

was obtained with the DIC technique. The results also explained why there were negative strains in the DIC results: For the experiment, the initial T-peel state was set as the reference state, and thus, the initial strain was 0, although it was not 0 for the bent part, as shown in Figure 12(b). Hence, there were negative strains observed when the local unloading occurred.

The strain distribution in this simulation study was a little different from the DIC results in ref. 4. The simulated strain distribution is shown in Figure 15. For the TPU coating, the strain at the end of the squeezed-out part of the TPU was much smaller relatively than that at the root of the peeling arm; however, this was not captured by the DIC results. The reason for that was that the width of the welded seam was very narrow, and the size of the sprayed speckles may also have not been small enough. These facts made it difficult for the cameras to record the details of the deformation there; this resulted in a calculation error with the DIC technique. In addition, the size of the squeezed-out part of the TPU of the experimental samples may not have been as large as the simulation model, and this also

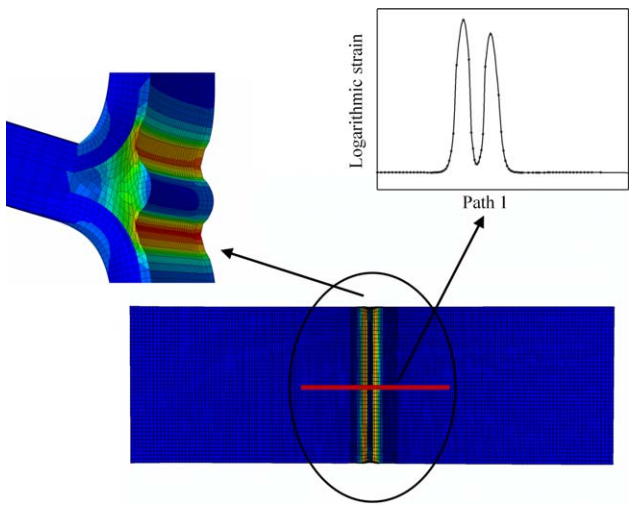

Figure 15. Strain distribution surrounding the seam area. [Color figure can be viewed in the online issue, which is available at wileyonlinelibrary.com.]

affected the measurement results. In sum, the simulation results indicate that the deformation within the seam area needed to be observed at the microscale.

CONCLUSIONS

A simple and reliable FE method within engineering has been presented to analyze the T-peel behavior of flexible composite films. The coating was modeled as hyperelastic, and the weaving method of the fabric was taken into account by modeling it as orthotropic. The friction among the yarns was neglected. The coating and the fabric were considered as a whole system, and they were assumed to have the same strain; the friction between them was also neglected. We found that the welding process caused no significant change in the constitutive law of the welded zone. Hence, the melted and remixed TPU coatings shared the same stress–strain relationship with the parent material. The numerical load–displacement curve predicted by the simulation work agreed well with the experimental results, and the stress–strain conditions surrounding the seam area was further investigated in detail. The maximum stress–strain occurred at the root of the peeling arm, which was located at the joint of the squeezed-out part of the TPU coatings and the parent material, and at the interface of the fabric and the coatings. Thus, fracture occurred more easily at these places; this was consistent with the experimental observations.

REFERENCES

1. Kabche, J. P.; Peterson, M. L.; Davids, W. G. *Compos. B* **2011**, *42*, 526.
2. Kawashita, L. F.; Kinloch, A. J.; Moore, D. R.; Williams, J. G. *Eng. Fract. Mech.* **2006**, *73*, 2304.
3. Nase, M.; Zankel, A.; Langer, B.; Grellmann, W.; Poelt, P. *Polymer* **2008**, *49*, 5458.
4. Yang, Y. B.; Zeng, P.; Lei, L. P.; Xu, Y. J. *Polym. Eng. Sci.* [Online early access]. DOI: 10.1002/pen.23875. Published Online: March 12, **2014**.
5. Thouless, M. D.; Yang, Q. D. *Int. J. Adhes. Adhes.* **2008**, *28*, 176.
6. Cavalli, M. N. Ph.D. dissertation, University of Michigan, **2003**.
7. Hadavinia, H.; Kawashita, L.; Kinloch, A. J.; Moore, D. R.; Willams, J. G. *Eng. Fract. Mech.* **2006**, *73*, 2324.
8. Pollitt, J. *J. Text. Institute Proc.* **1949**, *40*, 11.
9. Kato, S.; Yoshino, T.; Minami, H. *Eng. Struct.* **1999**, *21*, 91.
10. Kawabata, S.; Niwa, M.; Kawai, H. *J. Text. Inst.* **1973**, *64*, 21.
11. Pargana, J. B.; Lloyd-Smith, D.; Izzuddin, B. A. *Eng. Struct.* **2007**, *29*, 1323.
12. Hollande, S.; Laurent, J.; Lebey, T. *Polymer* **1998**, *39*, 5343.
13. Jones, P. L. High frequency heating [Online]. http://www.thermopedia.com/content/850/. **2011**, DOI: 10.1615/AtoZ.h.high_frequency_heating.
14. Yang, Q. S.; Jiang, Y. N. Analysis and design of tensioned cable-membrane structures; Beijing: Science press: Beijing, 2004; Chapter 3, pp 42.
15. Qi, H. J.; Boyce, M. C. *Mech. Mater.* **2005**, *37*, 817.